THE JOURNAL OF BIOLOGICAL CHEMISTRY VOL. 286, NO. 36, pp. 31250–31262, September 9, 2011

Environmental and Biofilm-dependent Changes in a *Bacillus cereus* Secondary Cell Wall Polysaccharide*[S]

Received for publication, April 12, 2011, and in revised form, July 21, 2011 Published, JBC Papers in Press, July 22, 2011, DOI 10.1074/jbc.M111.249821

Thomas Candela[‡§1,2], Emmanuel Maes[¶‖1], Estelle Garénaux[¶‖], Yoann Rombouts[¶‖], Frédéric Krzewinski[¶‖], Michel Gohar[‡], and Yann Guérardel[¶‖3]

From the [¶]Université de Lille1, Unité de Glycobiologie Structurale et Fonctionnelle, F-59650 Villeneuve d'Ascq, France, [‖]CNRS, UMR 8576, F-59650 Villeneuve d'Ascq, France, [‡]Micalis, INRA (UMR1319), Biofilms and Régulation Génétique chez les Bacillacées, Domaine de Vilvert, 78352 Jouy-en-Josas, France, and [§]Micalis, INRA (UMR1319), Génétique Microbienne and Environnement, Domaine de Vilvert, 78352 Jouy-en-Josas, France

Bacterial species from the *Bacillus* genus, including *Bacillus cereus* and *Bacillus anthracis*, synthesize secondary cell wall polymers (SCWP) covalently associated to the peptidoglycan through a phospho-diester linkage. Although such components were observed in a wide panel of *B. cereus* and *B. anthracis* strains, the effect of culture conditions or of bacterial growth state on their synthesis has never been addressed. Herein we show that *B. cereus* ATCC 14579 can synthesize not only one, as previously reported, but two structurally unrelated secondary cell wall polymers (SCWP) polysaccharides. The first of these SCWP, →4)[GlcNAc(β1–3)]GlcNAc(β1–6)[Glc(β1-3)][ManNAc(α1–4)]GalNAc(α1–4)ManNAc(β1→, although presenting an original sequence, fits to the already described the canonical sequence motif of SCWP. In contrast, the second polysaccharide was made up by a totally original sequence, →6)-Gal(α1–2)(2-R-hydroxyglutar-5-ylamido)Fuc2NAc4N(α1-6)GlcNAc(β1→, which no equivalent has ever been identified in the *Bacillus* genus. In addition, we established that the syntheses of these two polysaccharides were differently regulated. The first one is constantly expressed at the surface of the bacteria, whereas the expression of the second is tightly regulated by culture conditions and growth states, planktonic, or biofilm.

The cell wall surrounding cytoplasmic membrane is of prime importance in bacteria survival and adaptation to their environment. In Gram-positive bacteria, the cell wall includes a thick multilayer peptidoglycan to which most often are associated other cell-surface structures called secondary cell wall polymers (SCWPs)[4] (1). These secondary cell wall polymers include lipoteichoic acids anchored in the outer leaflet of plasmic membrane as well as teichoic acids, teichuronic acids, or neutral polysaccharides (SCWP polysaccharides), which are covalently bound, through a phosphodiester link, to the *N*-acetyl muramic acid moieties of the peptidoglycan. SCWPs are essential in *Bacillus subtilis* and were shown to be involved in the bacterial virulence in *Staphylococcus aureus* (2). In addition, SCWPs bind SLH (S-layer homology) domains containing proteins, thus anchoring them non-covalently to the cell wall (3). These proteins are involved in various functions, including peptidoglycan maturation (4, 5), binding to host tissues (6), or protein degradation (7). Teichoic acids and the secondary cell wall polysaccharide were also reported to be involved in biofilm formation (8–10).

Biofilms are multicellular structures attached to a solid or a liquid surface and embedded in a self-produced matrix. This matrix is made of polymers, mostly polysaccharides, DNA, and/or proteins, provides cohesion to the bacterial community (11–13), and acts as a shield, protecting bacteria within the biofilm. Biofilms are, therefore, persistent structures, resisting desiccation, cleaning procedures, and antimicrobial substances (14), which makes them a challenge in human health and industrial processes. Several species from the *Bacillus* genus, including *B. subtilis*, *Bacillus cereus* and *Bacillus anthracis*, have been identified to form biofilms in a wide range of different environments (15–17). In *B. cereus*, the formation of biofilms is enhanced by low nutrient supplies and requires the presence of biosurfactants (18). *B. cereus* is a Gram-positive, spore-forming bacterium, genetically close to *Bacillus thuringiensis*, a pathogen of insects used in crop protection, and to *B. anthracis*, a lethal pathogen of mammals previously used as a weapon in bioterrorism acts. This bacterium is an opportunistic pathogen frequently diagnosed in gastroenteritis cases (19) but also involved in other human diseases, including endophthalmitis and meningitis (20). It produces a high number of virulence factors, most of them controlled by a master virulence regulator (21). In addition, spores and biofilms produced by *B. cereus* are persistent contaminants of the food industry equipment (22).

B. cereus cell surface displays teichoic acids and secondary cell wall polysaccharides (23–26). These secondary cell wall polysaccharides were suggested to represent in this bacterium and its close relatives a virulence-associated carbohydrate anti-

* This work was supported by the Conseil Régional Nord-Pas de Calais ARCir (to Y. G.), the Ministère de l'Enseignement Supérieur (to Y. R.), and the Région Île de France (to T. C.). Research on the 800 and 900 MHz spectrometers was supported by the TGE RMN THC Fr3050.

[S] The on-line version of this article (available at http://www.jbc.org) contains supplemental Figs. S1–S7.

[1] Both authors equally contributed to this study.

[2] Present address: Faculté de Pharmacie ParisXI sud, EA 4043-Ecosystème Microbien Digestif and Santé, Chatenay Malabry 92290, France.

[3] To whom correspondence should be addressed. E-mail: yann.guerardel@univ-lille1.fr.

[4] The abbreviations used are: SCWP, secondary cell wall polymer; PS, polysaccharide; Ch HF-PS, for charged HF-PS; Ne HF-PS, neutral HF-PS; TOCSY, total correlation spectroscopy; HMBC, heteronuclear multiple bond coherence; DATDH, diaminotrideoxyhexose; HR-MAS, high resolution magic angle spinning; HCT, hydrolysate of casein Tryptone; BHI, brain heart infusion; HSQC, heteronuclear single quantum correlation.

gen motif (23). The exact structures of the secondary cell wall polysaccharides from two *B. cereus* strains were recently compared with those of *B. anthracis* Ames after their release from the cell wall using aqueous hydrogen fluoride (HF). The detailed analysis of the peptidoglycan HF-labile fractions established the occurrence of the consensus sequence (α-HexNAc-β-ManNAc-β-GlcNAc) in all three strains (24, 27). In particular, the backbone of the secondary cell wall polysaccharides isolated from *B. anthracis* Ames and *B. cereus* 10987 were shown to be composed of structurally related trisaccharide repeating units differentially substituted by a strain-specific pattern of α- and β-D-galactosidase residues. In comparison, *B. cereus* 14579 strain appears to synthesize similar but more complex polysaccharides containing the consensus trisaccharide sequence, the structure of which is, however, still elusive (24).

Although much information is currently available on the structure of cell wall-associated components, including teichoic acids and secondary cell wall polysaccharides, nothing is currently known about the evolution of these components in *B. cereus* and relatives species along the bacterial growth and in particular during the transition between planktonic and biofilm modes of life. Previous reports established, however, that growth conditions may influence their cell wall compositions. Particularly, in *B. subtilis*, teichoic acids are replaced by teichuronic acids during phosphate starvation (28). Such structural modifications of the bacterial cell wall may have an influence on the overall physicochemical properties of the cell surface that regulate bacterial interactions with substratum. Here we investigated the changes undergone by the secondary cell wall polysaccharide in the *B. cereus* ATCC 14579 strain during bacterial exponential and stationary growth and between bacteria in planktonic or in biofilm states. We first established that the polysaccharide fraction released by HF from *B. cereus* strain ATCC 14579 grown in planktonic conditions was composed of two distinct polysaccharides presenting very different structural features. Whereas one presented strong similarities with HF-released polysaccharide (HF-PS) isolated from *B. cereus* 10987 (24), the other one exhibited totally original structural features. Then, we demonstrated that these two polysaccharides were differentially regulated along the growth of bacteria in the biofilm phase but not in the planktonic phase.

EXPERIMENTAL PROCEDURES

Bacterial Strains and Culture Conditions—Biofilms were produced as floating pellicles with the *B. cereus* ATCC 14579 strain in HCT medium (29) at 37 °C in glass tubes (30) or in 50-ml beakers. Biofilms in 50-ml beakers were obtained in the same way as in glass tubes. Planktonic cultures were performed with the ATCC14579 strain in HCT or in BHI culture media at 37 °C and 175 rpm. In HCT, planktonic cultures were harvested at 5, 10, 15, and 20 h post-inoculation, and biofilms were harvested at 28, 48, 72, and 96 h post-inoculation. These timescales spanned the whole life of ATCC14579 planktonic cultures or biofilms in a poor medium. Planktonic cultures in BHI (a rich medium) were harvested at an optical density of 4.0 (6 h post-inoculation).

Preparation of Polysaccharide Fractions—Secondary cell wall polymers were extracted similarly to the peptidoglycan (31), with an additional hydrolysis step using hydrofluoric acid. The bacterial cells, harvested from planktonic cells or from biofilms, were boiled for 10 min in 40 ml of (50 mM Tris-HCl, pH 7.4, 150 mM NaCl, 1% SDS) and spun down at 6500 × *g* for 10 min. This step was repeated once to obtain only the peptidoglycan together with its covalently linked secondary cell wall polymers. The resulting pellet was washed in 40 ml of 50 mM Tris, pH 7.4, sonicated, and centrifuged at 50,000 × *g* for 20 min. The remaining contaminants were discarded by treating the resulting pellet, solubilized in 20 mM $MgSO_4$, successively by DNase (1 mg/ml) and RNase (5 mg/ml), then by proteinase K (20 μg/ml at room temperature for 12 h) in the presence of 10 mM $CaCl_2$, and finally by SDS (1% at 100 °C for 10 min.). The insoluble material, recovered after centrifugation at 50,000 × *g* for 20 min, was rinsed in pure water and treated successively with 8 M $LiCl_2$ and with 100 mM EDTA. The resulting insoluble material, spun down at 50,000 × *g* for 20 min, was rinsed twice in pure water, and digested with 46% hydrofluoric acid for 48 h at room temperature. After centrifugation at 20,000 × *g* for 10 min, the supernatant containing the secondary cell wall polymers was precipitated with 3 volumes of ethanol. The precipitate was then dried and stored at −20 °C until use.

Mild Hydrolysis of Polysaccharide Fractions—Total polysaccharide fraction was hydrolyzed repetitively under mild conditions (0.1 M trifluoroacetic acid at 80 °C for 1 h). After each hydrolysis step, four volumes of ethanol were added, and the liberated oligosaccharides were collected in the ethanol fraction. Release of oligosaccharides from total polysaccharide was assessed by TLC analysis on silica gel using butanol/acetic acid/H_2O (40/30/20) as solvent. Completeness of the reaction was assessed by dosing carbohydrate by phenol-sulfuric staining and weighing of the ethanol soluble fraction. Typically, four hydrolysis steps were sufficient to liberate all hydrolysable material. Oligosaccharides were further purified by gel filtration on a Bio-Gel P-2 column.

Anion Exchange Chromatography of Polysaccharide—Total polysaccharide was fractionated into a neutral and an anionic fraction on a HPLC apparatus fitted with a strong anion exchange column Mono Q (Amersham Biosciences). The sample was loaded and eluted with a flow rate of 0.5 ml/min with 20 mM Tris-HCl (pH 8.0) followed by a NaCl gradient (0–10 min, 0 M; 10–60 min, 0–0.6 M; 60–65 min, 0.80 M) in 20 mM Tris-HCl (pH 8.0).

Glycosyl Linkage Analysis—Linkage analyses of monosaccharides were achieved by permethylation followed by hydrolysis, reduction, and derivatization with acetyl groups. Briefly, samples were permethylated according to Ciucanu (32), hydrolyzed in 4 M trifluoroacetic acid for 4 h at 100 °C, and then reduced with sodium borohydride in 0.05 M NH_4OH for 4 h. Reduction was stopped by dropwise addition of acetic acid until pH 6 was reached, and borate salts were co-distilled by repetitive evaporation in dry methanol. Partially methylated, reduced monosaccharides were acetylated in 500 μl of acetic anhydride at 100 °C for 2 h. Solution was dried and partially methylated, and acetylated reduced monosaccharides were extracted three times in chloroform.

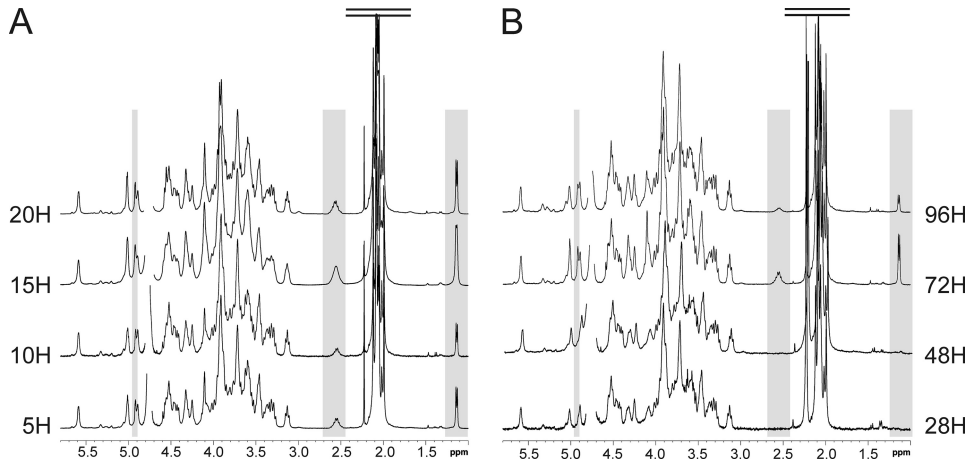

FIGURE 1. **Structural mapping of HF-PS isolated from planktonic and biofilm phases of *B. cereus* ATCC 14579.** ^{1}H NMR spectra of HF-PS from planktonic (*A*) and biofilm (*B*) phases at four different growth times are shown. Spectra from all planktonic time points were identical, whereas spectra from early (28 and 48 h) differed from late biofilms (72 and 96 h). Three easily identified signals at 4.91, 2.52, and 1.13 ppm that show variations along growth times are highlighted in *gray*.

NMR Analysis—After two exchanges with $^{2}H_2O$ (Eurisotop-Saclay France), sample was dissolved in pure D_2O. Experiments were recorded at various temperatures (280, 300, 343 K), but only spectra recorded at 300 K are shown. The pD was kept neutral. Experiments were recorded on Bruker spectrometers at three different fields. 9.4, 18.8, and 21.6 tesla were ^{1}H-resonated at 400.33, 800.12, and 900.11 MHz but ^{13}C-resonated at 100.2, 200.3, and 220.0 MHz, respectively. ^{31}P spectrum was recorded at 9.4 tesla. Pulse programs used were extracted from Bruker pulse program library where pulses and delays were optimized for each experiment. For TOCSY experiments, 40, 60, 80, and 100 ms were used for mixing time in spectra recording.

HR-MAS NMR experiments were achieved on an 18.8 T Avance II Bruker spectrometer. The experiments were acquired with a ^{13}C,^{1}H/^{31}P/^{2}H probe with uniaxial gradients. Before analysis, cell-pellets were washed twice with deuterium oxide (Euriso-top, Gif-sur-Yvette, France). The 4-mm ZrO_2 rotors (CortecNet, Paris, France) were filled with 50 μl of cell pellets including 0.5 μl of acetone as the internal standard and finally centrifuged at 3000 rpm. All spectra were recorded at 293 K, and the rotor spinning rate was 8 kHz. All experiments came from the Bruker library pulse program, and delays and powers were optimized for each. For ^{13}C,^{1}H HSQC, the spectral widths were 12.820 Hz (^{1}H) with 1.024 points for free induction decay resolution and 29.994 Hz (^{13}C) for 400 scans, giving 12.5 and 75.0 Hz/point respectively.

Mass Spectroscopy—MALDI-MS and MS/MS analyses of polysaccharides were performed on 4800 Proteomics Analyzer (Applied Biosystems, Framingham, MA) mass spectrometer, operated in the reflectron mode. For MS acquisition, 5 μl of diluted samples in H_2O were mixed with 5 μl of 2,5-dihydroxybenzoic acid matrix solution (10 mg/ml dissolved in H_2O/CH_3OH (1:1, v/v)). The mixtures (2 μl) were then spotted on the target plate and air-dried. Peaks observed in the MS spectra were selected for further MS/MS. Collision-induced dissociation MS/MS data comprise a total of 100 subspectra of 3000 laser shots. Two or more spectra can be combined post-acquisition with mass tolerance set at 0.1 Da to improve the signal-to-noise ratio. The potential difference between the source acceleration voltage and the collision cell was set to 1 kV, and argon was used as the collision gas.

RESULTS

Comparison of Polysaccharides—In a first approach, polysaccharides were released by aqueous hydrogen fluoride from different growth times between 5 and 20 h or between 28 and 96 h post-inoculation for planktonic and biofilm cultures, respectively, then analyzed by ^{1}H NMR. As observed on Fig. 1, growth time did not have any visible influence on polysaccharide structure in planktonic phase, whereas it did in the biofilm phase. In particular, polysaccharides extracted from early (28 and 48 h) and late (72 and 96 h) biofilms exhibited different NMR spectra. Surprisingly, spectra from late biofilms were identical to all planktonic polysaccharides, whereas early biofilms showed identical simpler spectra. These were characterized by the disappearance of many NMR signals, in particular the easily observed signals at 4.91, 2.52, and 1.13 ppm, all other signals being identical. Thus, to appreciate the origin and the extent of the structural modifications that take place in the surface polysaccharide during biofilm growth, we first focused our study on the structural elucidation of the complex polysaccharide expressed in planktonic and late biofilm phases.

Analysis of the Planktonic Phase Polysaccharide—A ^{13}C,^{1}H HSQC NMR experiments of total polysaccharide isolated from 5–20 h planktonic phase permitted identification of nine anomeric signals (**I** to **IX**) out of which four were tentatively assigned to α anomers ($^{1}J_{H,C} \sim 170$ Hz, **I**, **II**, **IV**, **V**) and five to β anomers ($^{1}J_{H,C} \sim 160$ Hz, **III**, **VI**, **VII**, **VIII**, **IX**) (Fig. 2*A*). Furthermore, eight ^{13}C,^{1}H signals were assigned to *N*-acetylated or *N*-acylated carbons according to their high field deshielded NMR parameters (Fig. 2*D*). These were later assigned as C2 of residues **I**, **III**, **IV**, **V**, **VI**, **VII**, and **VIII** as well as C4 of **I** residues by two-dimensional ^{1}H,^{1}H NMR experiments. Altogether, these experiments established the presence of nine monosaccharides, out of which seven were assigned to *N*-acetylated hexosamines and two to neutral hexoses. However, total assignment of individual spin systems was delicate at this stage of the

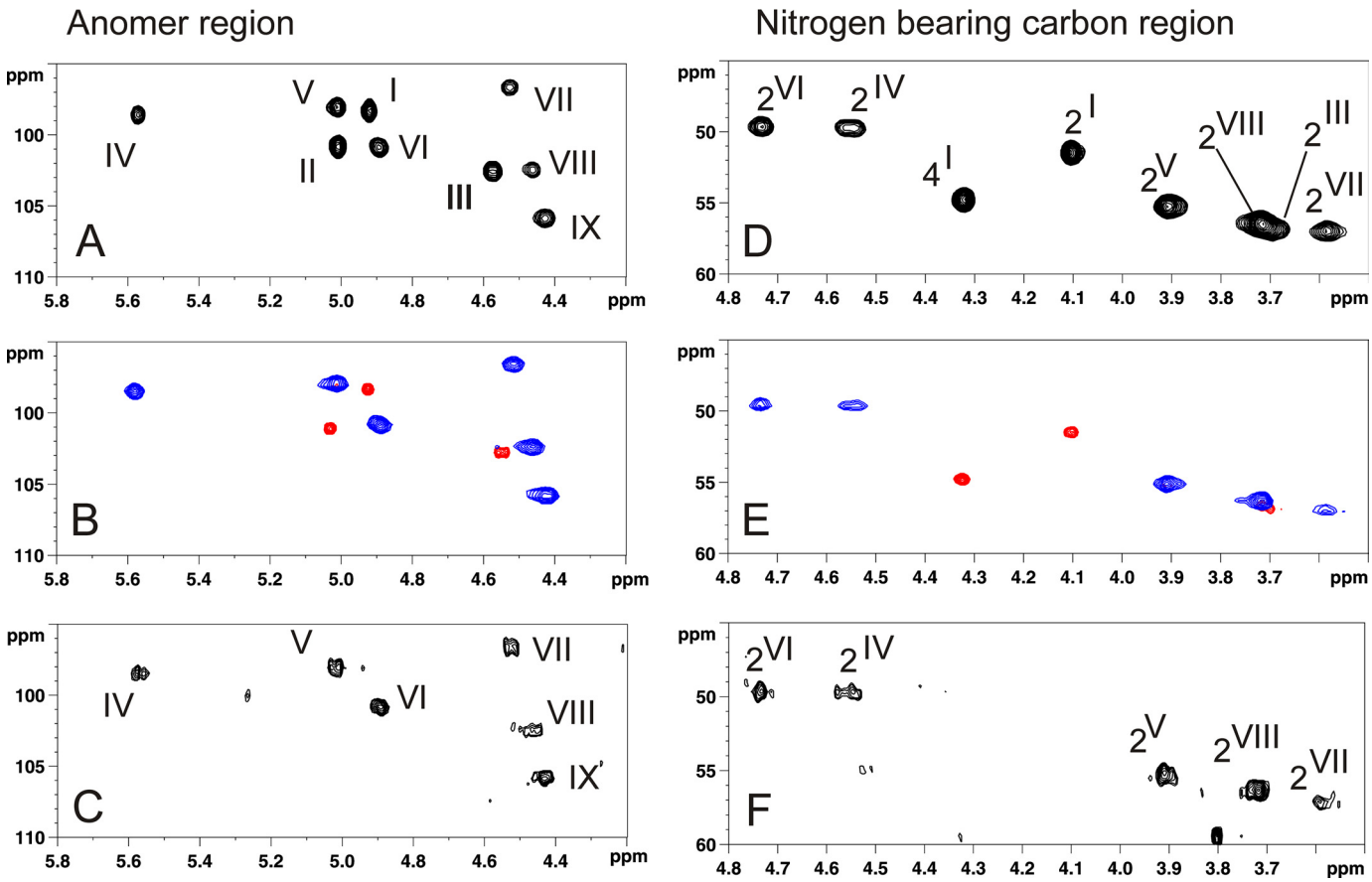

FIGURE 2. **$^{13}C,^{1}H$ HSQC NMR spectra of HF-PS from planktonic and biofilm phases of *B. cereus* ATCC 14579.** Shown are the anomer regions (*A–C*) and nitrogen-bearing carbon regions (*E–F*) of $^{13}C,^{1}H$ HSQC spectra of intact HF-PS from planktonic phase (*A* and *D*), Ne HS-PS and Ch HF-PS fractions generated by mild hydrolysis from planktonic phase (*B* and *E*), and 24-h biofilm phase (*C* and *F*). In *B* and *E*, *blue* signals correspond to Ne HS-PS ,and *red* signals to Ch HF-PS from planktonic phase.

study because of numerous overlaps of anomeric signals both in the proton (**II** and **V**; **I** and **VI**; **VII** and **VIII**) and in the carbon (**I**, **IV**, and **V**; **II** and **VI**; **III** and **VIII**) dimensions (Fig. 2*A*). Thus, to simplify the NMR spectra and gain access to its fine structure, we separated the total polysaccharide in two fractions using two different strategies (Fig. 3*A*).

Fractionation of Polysaccharide—The first strategy consisted of separating the native polysaccharides by strong anion exchange chromatography assuming that the total polysaccharide was constituted by two distinct macromolecules. As shown on Fig. 3*B*, the elution profile of intact polysaccharide on a strong anion exchange chromatography column by a gradient of sodium chloride generated two fractions; that is, one non-retained fraction and one retained fraction that were further individually analyzed. As will be explained in the following chapters, the retained polysaccharide, called Ch HF-PS for charged HF-PS, included one free carboxyl group that conferred a negative charge, whereas the non-retained polysaccharide was devoid of acidic group and was thus called Ne HF-PS for neutral HF-PS.

The second strategy consisted of repetitively hydrolyzing the polysaccharide in mild acid conditions to generate two fractions, one acid stable and one acid labile. Liberated oligosaccharides were extracted by ethanol after each hydrolysis step, whereas the non-labile fraction was submitted to another hydrolysis step. These conditions, which were devised to maximize liberation of acidic labile domain as repeating units by preserving the acidic resistant domain, have been previously successfully used to generate fucosylated oligosaccharides from sponge polysaccharides (33). Mild acid hydrolysis of intact polysaccharide (HF-PS) permitted the generation of two fractions presenting different solubility in 70% alcohol solution (Fig. 3*A*). The stepwise monitoring of hydrolysis process showed that five hydrolysis steps were enough to cleave and liberate as an ethanol-soluble fraction all the acid labile fraction from the total polysaccharide, which represented about 70% of the initial polysaccharide (Fig. 3*C*). Structural analysis of acid stable and acid labile fractions (see after) showed that these two fractions presented identical structural features to Ne HF-PS and Ch HF-PS separated by anion exchange chromatography, albeit the depolymerization of Ch HF-PS after acid hydrolysis. Thus both strategies lead to the separation of HF-PS in two distinct fractions, Ne HF-PS and Ch HF-PS.

As shown in Fig. 2, *B* and *E*, Ch HF-PS and Ne HF-PS exhibited totally different $^{13}C,^{1}H$ HSQC NMR spectra, establishing that they were devoid of any trans-contaminating material. Comparison of all fractions (Fig. 2) showed that the $^{13}C,^{1}H$ HSQC NMR spectrum of total HF-PS from planktonic phase is the result of the combination of Ch HF-PS and Ne HF-PS subspectra. Individual signal assignments established that Ch

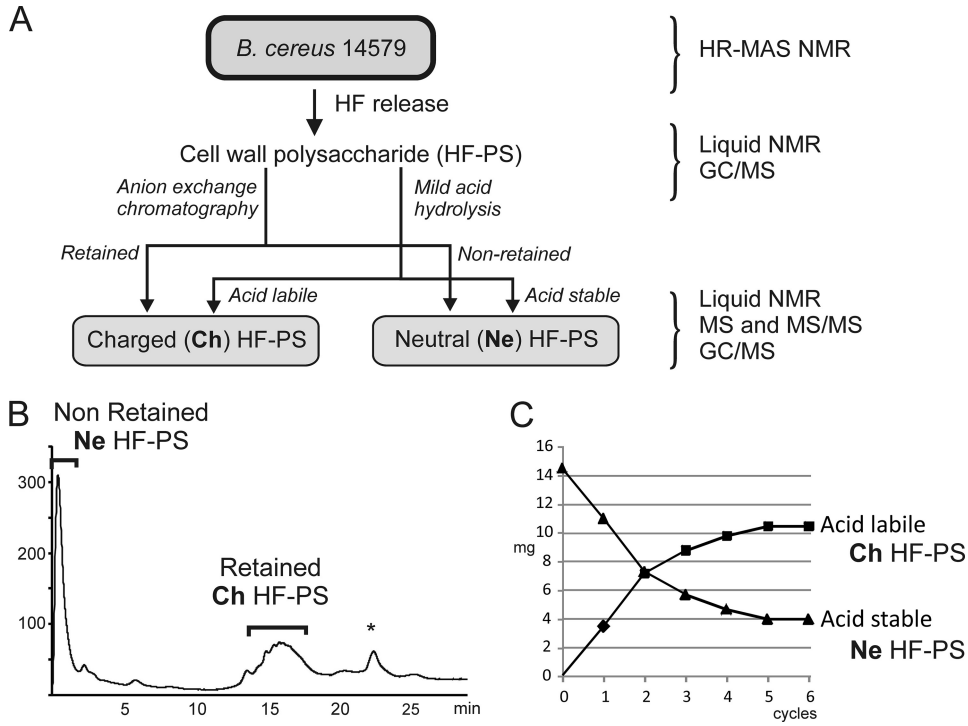

FIGURE 3. **Purification schemes of HF-PS components.** Two distinct components were separated using two different procedures. *A*, Ch HF-PS and Ne HF-PS were purified from total HF-PS by either mild acid hydrolysis or anion exchange chromatography. *B*, anion exchange chromatography separated a charged retained fraction (Ch HF-PS) from a neutral non-retained fraction (Ne HF-PS). *C*, mild acid hydrolysis followed by ethanol precipitation generated an acid labile fraction from an acid stable fraction, which subsequent structural analysis identified as Ch HF-PS and Ne HF-PS, respectively. The efficiency of acid hydrolysis was monitored along the hydrolysis steps (*C*). All purified fractions, as well as total HF-PS and intact *B. cereus* cells were analyzed by different combinations of analytical methods. *, contaminant non-carbohydrate signal.

HF-PS consisted of three monosaccharide units (signals **I** to **III**) and Ne HF-PS of six units (**IV** to **IX**). Separation of polysaccharide in two fractions resolved most of the overlapping NMR signals and further enabled an exact interpretation of spectra of individual polysaccharides. Unexpectedly, we observed that **II**-H1 and III-H1chemical shifts slightly changed when Ch HF-PS was analyzed alone (**II**-H1 $\Delta\delta$ + 0.024; **III**-H1 $\Delta\delta$ −0.028) or in a mixture with Ne HF-PS. Although this phenomenon was never reported to our knowledge, we suggest that these variations arose from sugar-sugar interaction phenomena in a similar fashion that is observed during protein-protein interactions (34).

Altogether, these data strongly suggested that the total SCWP polysaccharide was constituted by two independent polysaccharides; one charged and acid labile polysaccharide (Ch HF-PS) and another neutral and acid stable polysaccharide (Ne HF-PS). Structural analysis of these two polysaccharides will permit (1) the establishment of the nature of the structural differences between polysaccharides and (2) determine whether the structural differences between phases arise from the modification of a common polysaccharide core or from the specific induction of the two different polysaccharides.

Analysis of Neutral Polysaccharide Ne HF-PS—Six anomer signals (**IV** to **IX**) were identified on the $^{13}C,^{1}H$ HSQC spectrum of Ne HF-PS, establishing the presence of six different monosaccharide units, out of which five appeared to be hexosamines, according to the observation of five *N*-acetylated C2 signals between 49 and 57 ppm (**IV**- to **VIII**-C2). The nature of individual monosaccharides was established by a combination of NMR analysis of polysaccharide and gas chromatography analysis of partially methylated and acetylated reduced monosaccharides. In particular, spin systems of all units were assigned by NMR analysis using two-dimensional COSY, TOCSY, nuclear Overhauser effect spectroscopy (NOESY), HSQC (decoupled or not), and HMBC experiments, and sequencing information was obtained by $^{1}H,^{1}H$ NOESY and $^{13}C,^{1}H$ HMBC experiments.

Large $^{1}J_{H,C}$ coupling constant (178 Hz) and the deshielded **IV**-H1 value at 5.588 ppm established that **IV** unit exhibited an α configuration. Then, the total spin system and the $^{1}H,^{1}H$ vicinal coupling constant pattern of **IV** in which $^{3}J_{H1,H2}$, $^{3}J_{H2,H3}$, $^{3}J_{H3,H4}$, and $^{3}J_{H4,H5}$ were small (S), large (L), S and S (S/L/S/S) showed that this residue had an α-*galacto* configuration (35). Finally, the upfield chemical shifts of **IV**-H2/C2 at δ 4.551/49.72 and the presence of an *N*-acetamido group at 1.999/23.62 ppm demonstrated that **IV** was an α-GalNAc residue (Table 1, Fig. 4). Deshielding of **IV**-C3, -C4, and -C6 chemical shift values at δ77.1, 75.2, and 68.6 compared with unsubstituted α-GalNAc residue (C3, $\Delta\delta$ + 8.5; C4, $\Delta\delta$ +5.5, and C6, $\Delta\delta$ +6.2) established that **IV** residue was trisubstituted in C3, C4, and C6 positions, in accordance with the splitting of H6 and H6′ signals at 3.907 and 3.636 ppm (36). The presence of this unusual trisubstituted GalNAc residue was confirmed by linkage analysis in gas chromatography coupled to mass spectrometry (supplemental Fig. S1). Similarly, despite the strong coupling constant that prevented the attribution of vicinal $^{3}J_{H1,H2}$ and $^{3}J_{H2,H3}$ coupling constants, the unit **VI** could be assigned to a β-D-ManNAc unit based on the attribution of the spin system and of the

TABLE 1
Proton and carbon chemical shifts (ppm) of Ne HF-PS
Values in parentheses correspond to direct coupling constant ($^1J_{H,C}$) between ^1H and ^{13}C of anomer position. Bold values correspond to carbon-bearing substitution.

		Chemical shifts						
		ppm						
Residues		1	2	3	4	5	6/6′	NAc
α-Gal*p*NAc (**IV**)	^1H	5.588	4.551	3.956	4.258	4.086	3.907/3.636	1.999
	^{13}C	98.5 (~178 Hz)	49.72	**77.08**	**75.20**	71.3	**68.60**	23.62
α-Man*p*NAc (**V**)	^1H	5.021	3.915	3.911	3.610	4.323	~3.9/3.7	2.092
	^{13}C	98.04 (~172Hz)	55.20	71.64	70.72	72.62	~62	23.62
β-ManpNAc (**VI**)	^1H	4.897	4.740	4.538	3.855	3.570	3.99/3.66	2,092
	^{13}C	100.93 (~164Hz)	49.63	**75.8**	70.1	76.3	62.4	23.62
β-Glc*p*NAc (**VII**)	^1H	4.521	3.592	3.480	3.298	3.473	3.99/3.66	2.064
	^{13}C	96.6 (~160Hz)	57.0	75.8	72.1	77.4	62.4	23.62
β-Glc*p*NAc (**VIII**)	^1H	4.471	3.721	3.721	3.721	3.55	3.99/3.66	2.125
	^{13}C	102.5 (~163Hz)	56.4	**80.3**	**73.6**	75.4	62.4	23.62
β-Glc*p* (**IX**)	^1H	4.428	3.139	3.473	3.350	3.55	3.99/3.66	no
	^{13}C	105.9 (~160Hz)	74.3	76.0	71.4	75.4	62.4	no

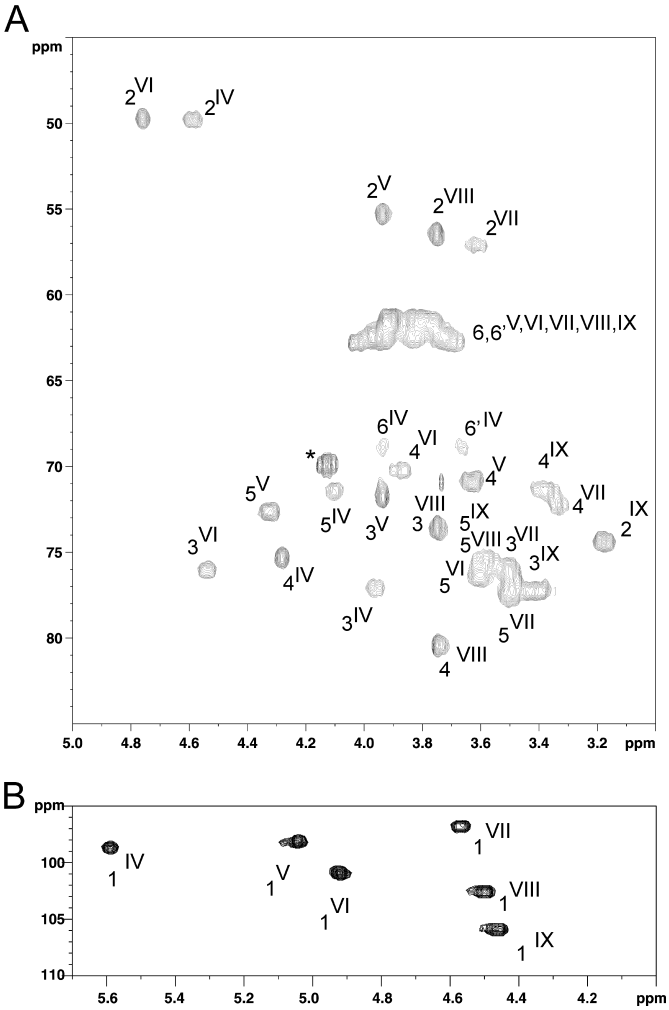

FIGURE 4. **$^{13}C,^1H$ HSQC NMR analysis of Ne HF-PS from planktonic phase.** Shown is $^{13}C,^1H$ HSQC NMR spectra of the bulk region (*A*) and anomer region (*B*) of Ne HF-PS.

remaining $^1H,^1H$ and $^{13}C,^1H$ coupling constant pattern. As for **IV**, observation of **VI**-C2 at 49.6 ppm and of *N*-acetyl group at δ 2.092/23.62 backed up its attribution to a hexosamine residue. Strong coupling constants also occurred between **VIII**-H2, -H3, and -H4 that resulted in identical chemical shifts for these three signals at 3.721 ppm irrespective of the experimental conditions. However, $^{13}C,^1H$ anomeric signal at δ 4.471/96.6 with $^1J_{H1,C1}$ of 163 Hz as well as the **VIII**-C2 signal at δ 56.4 typified that that unit was a β-*N*-acetylhexosamine unit. Such a strong coupling constants pattern is often observed for β-GlcNAc residues linked to α-HexNAc in C6 position. On this basis, we proposed that the **VIII** unit was a β-GlcNAc residue. Then, deshielded **VIII**-C3 and **VIII**-C4 signals at 80.3 and 73.6 ppm established that it was substituted in both positions in accordance with the observation of a 6-methyl-3,4-diacetyl-2-*N*-methyl-acetyl hexosaminitol residue in GC/MS (data not shown).

Strong inter-residue effects $^1J_{H1,C1}$ observed in rotating from Overhauser enhancement spectroscopy experiments demonstrated that **VIII** was linked to **IV**, **IV**, to **VI** and **VI** to **VIII**, which established the presence of a linear polysaccharide core composed of the repeating sequence **VIII**-**IV**-**VI** (supplemental Fig. S2). HMBC experiments permitted establishing the sequence **IV**(1–4)**VI**(1–4)**VIII** because of $^3J_{H,C}$ **IV**-H1/**VI**-C4 and **VI**-H1/**VIII**-H4 correlations (data not shown). Finally, a strong nuclear Overhauser effect between **VIII**-H1 and **IV**-H6 and H6′ showed that the **VIII** unit substituted **IV** in C6 position, establishing the sequence of the core polysaccharide from Ne HF-PS as →4)GlcNAc(β1–6)GalNAc(α1–4)ManNAc(β1→.

As established by the respective chemical shifts of **VIII**-C3, **IV**-C3, and **IV**-C4 at 80.3, 77.08, and 75.20 ppm, this trisaccharide unit is further substituted in three positions by the remaining yet unidentified residues **V**, **VII**, and **IX**. The configuration of unit **V** was determined using undecoupled $^{13}C,^1H$ HSQC, 1D selective ^1H TOCSY with various mixing times, $^1H,^1H$ two-dimensional COSY and TOCSY NMR experiments. $^1J_{H1,C1}$ coupling constant of 171 Hz and chemical shift of **V**-C2 at 55.20 ppm indicated that **V** was a 2-*N*-acetylated monosaccharide with an α-configuration. Then residue **V** was assigned to an α-ManNAc residue based on its $^3J_{H,H}$ S/S/L/L coupling constants pattern and attribution of total spin system. All carbons resonated like unsubstituted carbons (Table 1), establishing that **V** was a terminal non-reducing α-ManNAc residue. The unit **VII** was characterized as a β-GlcNAc residue based on the observation of total vicinal coupling constants on serial $^1H,^1H$ COSY and TOCSY spectra and of the direct coupling constant $^1J_{H,C}$ at 160 Hz. $^{13}C,^1H$ values established that **VII** is an unsubstituted β-GlcNAc residue present in terminal non-reducing end, unlike **VIII,** which is disubstituted in C3 and C4 positions (36). Finally, **IX** was easily identified as a terminal non-reducing

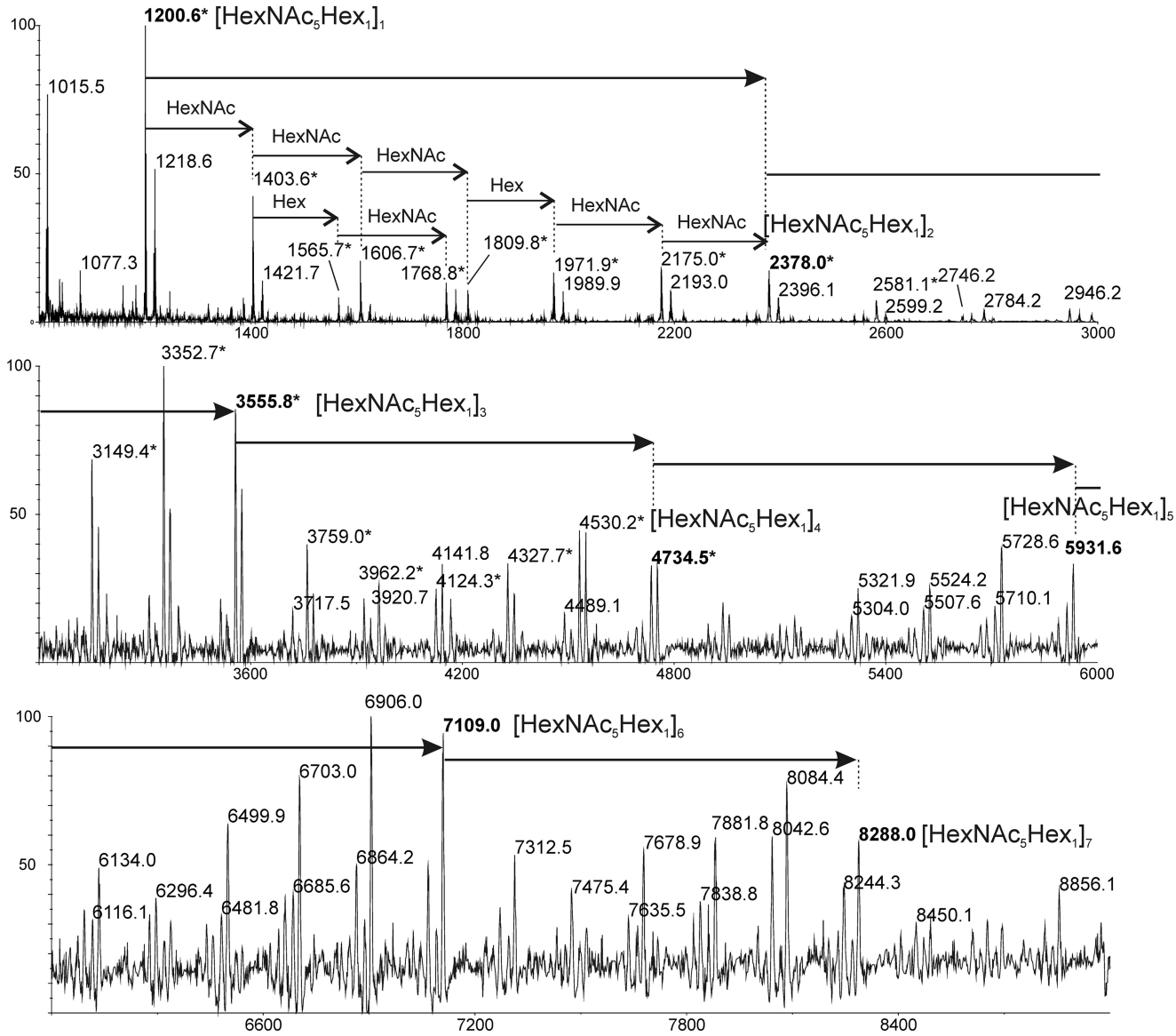

FIGURE 5. **Determination of the size distribution of Ne HF-PS from planktonic phase by MALDI-TOF-MS analysis.** MS analysis in positive mode permitted identification of polymers with $[M+Na]^+$ apparent molecular weights ranging from *m/z* 1218 to 8288. *, correspond to $[M+Na-18]^+$ oxonium type fragments generated by in source fragmentations of the polysaccharide core.

β-Glc residue because of its vicinal coupling constants pattern L/L/L/L and its $^{13}C,^{1}H$ spin system (Table 1). The substitution pattern of the **VIII**-**IV**-**VI** core repeating unit by residues **V**, **VII,** and **IX** was established by a combination of $^{1}H,^{1}H$ rotating frame Overhauser enhancement spectroscopy and $^{13}C,^{1}H$ HMBC NMR experiments (supplemental Fig. S2 and data not shown). A dense network of correlations including V-H1 → IV-H4, V-H1 → IV-C4, IX-H1 → IV-H3, IX-H1 → IV-C3, and VII-H1 → VII-H3 permitted deduction of the final structure of the hexasaccharide repeating unit of the neutral polysaccharide as [GlcNAc(β1–3)]GlcNAc(β1–6)[Glc(β1–3)][ManNAc(α1–4)]GalNAc(α1–4)ManNAc(β1–4).

The nature of this repeating unit was confirmed by mass spectrometry analysis. MALDI-TOF spectrum of Ne HF-PS showed a very complex profile characterized by a large number of signals between 794 and 8288 presenting *m/z* values intervals of either 203 or 162 atomic mass units, attributed to HexNAc and Hex, respectively (Fig. 5). All signals could be assigned to polymers containing from 6 (*m/z* 1200) to 42 (*m/z* 8288) monosaccharide (HexNAc and Hex) units. However, two sets of signals were identified; one corresponded to $[M+Na]^+$ adducts of HexNAc- and Hex-containing polymers ranging from *m/z* 1218 to 8288, the other to $[M+Na]^+$ oxonium-type adducts ranging from *m/z* 1200 to 4735 (Fig. 5). Oxonium types are believed to be generated by in-source fragmentations of the polysaccharide during high energy desorption from the MALDI matrix. Based on *m/z* calculations, a series of $[M+Na]^+$ signals at *m/z* 1218, 2396, 3574, 4753, 5931, 7110, and 8288 was assigned as polysaccharides containing from one to seven ($HexNAc_5Hex_1$) repeating units (Fig. 5). Similar oxonium-derived signals at *m/z* 1200, 2379, 3556, and 4735 were assigned to polysaccharide fragments containing up to four repeating units. In addition, many intermediate values signals with HexNAc or Hex increments were assigned. MS/MS fragmentation of the

TABLE 2
Proton and carbon chemical shifts (ppm) of Ch HF-PS
Values in parentheses correspond to direct coupling constant ($^1J_{H,C}$) between ^{1}H and ^{13}C of anomer position. Bold values correspond to carbon bearing substitution.

		Chemical shifts						
		ppm						
Residues		1	2	3	4	5	6/6′	NAc
α-FucpdiNAc (**I**)	^{1}H	4.915	4.104	4.102	4.323	4.295	1.132	2.077
	^{13}C	98.36 (~172 Hz)	51.49	68.29	54.80	66.90	17.05	23.52
α-Galp (**II**)	^{1}H	4.987	3.813	3.948	3.918	4.131	3.903/3.633	
	^{13}C	100.81 (~170Hz)	69.93	70.72	70.02	70.46	**68.19**	
β-GlcpNAc (**III**)	^{1}H	4.599	3.697	3.583	3.595	3.632	3.942/3.746	2.045
	^{13}C	102.52 (~162Hz)	56.91	73.39	70.92	75.63	**66.61**	23.38
2-OH glutarate (**OH-Glu**)	^{1}H		3.959	2.523	2.066			
	^{13}C	180.00	**80.72**	32.67	30.05	178.70		
α-FucpdiNAc (**I**[a])	^{1}H	4.91	4.09	4.09	4.29	4.28	1.13	2.12
	^{13}C	98.4	51.5	68.2	54.7	66.8	16.8	23.2
α-GlcpNAc (**III**[a])	^{1}H	5.25	3.89	3.76	3.61	3.97	3.96/3.66	2.05
	^{13}C	92.2	55.4	72.3	71.5	71.7	**67.2**	23.3
β-GlcpNAc (**III**[a])	^{1}H	4.73	3.66	3.58	3.56	3.57	3.96/3.66	2.05
	^{13}C	96.4	58	71.2	71.2	75.6	**67.2**	23.3

[a] Corresponds to the proton and carbon chemical shifts (ppm) of the disaccharide obtained by 4 M TFA hydrolysis of **Ch HF-PS** (supplemental Fig. S5).

single repeating unit at *m*/*z* 1200 demonstrated it is constituted by a linear HexNAc stretch substituted by a single HexNAc and a single Hex residue, in accordance with the structure established by NMR (supplemental Fig. S3).

Analysis of Charged Polysaccharide Ch HF-PS—After structural determination of the neutral polysaccharide, charged polysaccharide isolated from planktonic phase HF-PS was analyzed using similar techniques. The one-dimensional ^{13}C,^{1}H HSQC NMR spectrum (Fig. *2B*, supplemental Fig. S4) showed three anomer signals at 4.987 (**II**), 4.915 (**I**), and 4.599 (**III**), establishing the presence of three different types of monosaccharides. Unit **II** was identified as α-galactosyl residue on the basis of its coupling constants pattern observed on COSY and TOCSY spectra in accordance with Koërner *et al.* (35). Starting from **II**-H1 at 4.987 ppm (supplemental Fig. S4, Table 2) with a small (S) $^3J_{H1,H2}$ (~3 Hz), we observed a correlation at 3.813 ppm with a large (L) $^3J_{H2,H3}$ coupling constant indicating that H3 is in an axial position, whereas H4 (δ 3,918) is in an equatorial position as its $^3J_{H3,H4}$ is small and $^3J_{H4,H5}$ is small too. Finally, H6,6′ were identified on the ^{13}C,^{1}H HSQC spectrum (Fig. 6) as two distinct multiplets at δ^{13}C,^{1}H 3.903/68.2 and 3.633/68.2, indicating that **II** is O-6-substituted (36).

Unit **III** was identified as a β-*N*-acetyl-glucosamine residue. On COSY and ^{13}C,^{1}H HSQC spectra the anomeric proton ^{13}C,^{1}H signal at 4.599/102.52 ppm showed a $^1J_{H,C}$ of 162 Hz, indicating a β anomer (supplemental Fig. S4). Its proton coupling constants pattern revealed a L/L/L/L configuration, indicating a β-*gluco* configuration (Table 2). Moreover, the chemical shift of its C2 at 56.9, typical of a nitrogen-bearing carbon, and the presence of a *N*-acetyl group at 2.045 ppm proved its assignment as a β-GlcNAc residue. Finally, **III** was shown to be O-6-substituted according to their H6 and H6′ signals, resonating at 3.942 and 3.746 and bore by a deshielded carbon at 66.61 ppm.

Unit **I** ^{13}C,^{1}H spin system was more difficult to assign because its ring protons exhibited strong vicinal coupling constants, which generated very close chemical shifts, in particular for **I**-H2 and **I**-H3 signals as well as for **I**-H4 and **I**-H5 signals (Table 2). Individual assignment of ^{13}C,^{1}H signals established that C2 and C4 positions were substituted by nitrogen atoms based on their upfielded resonances at 51.5 and 54.8 ppm (36),

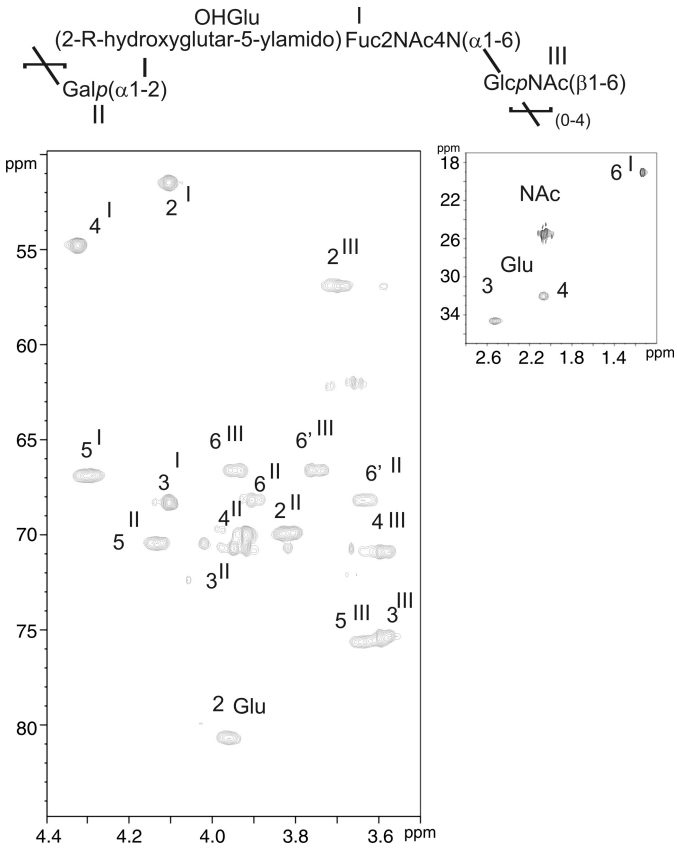

FIGURE 6. **^{13}C,^{1}H HSQC NMR analysis of the Ch HF-PS from planktonic phase.**

whereas C3 was unsubstituted (^{13}C at 70.8 ppm). Finally, H4 was coupled with a multiplet at ^{13}C,^{1}H 4.295/66.90 ppm assigned to H5 that was in turn coupled to a characteristic doublet of methyl group at δ 1.132/17.05. Altogether, these parameters established that **I** was a 2,4,6-tri-deoxy-2,4-diamino hexosamine, a bacillosamine-related diaminotrideoxyhexose (DATDH) previously described in *Neisseria meningitidis* (37). The presence of a *N*-acetyl signal at 2.077 ppm indicated that the C2 position was *N*-acetylated. Then a set of five NMR signals including two -COOH (^{13}C at 178.7 and 180 ppm), two -CH_2- (^{13}C,^{1}H at 2.066/30.05 and 2.523/32.67 ppm) and one

-CHOR- (^{13}C,^{1}H at 3.959/80.72 ppm) groups was associated to a glutaric acid group substituting the C4 position of DATDH, in accordance to previously published parameters (38) (Table 2). This glutarate (Glu) was shown to be attached on the DATDH through an *N*-acyl linkage on the four-amino group, due to the vicinal heteronuclear coupling constant ($^{3}J_{H,C}$) between **I**-H4 and Glu-C5 observed at δ 4.323/178.70 on the ^{13}C,^{1}H HMBC NMR spectrum (data not shown). The configuration of this monosaccharide could not be directly obtained from NMR spectra because of the strong ^{1}H-^{1}H coupling constants, probably generated by an unusual spatial conformation. To solve this problem, we hydrolyzed the supernatant in strong acidic conditions, hypothesizing that the cleavage of the polysaccharide to mono- or disaccharides would relax the molecular constraints and allow a measurement of ^{1}H-^{1}H coupling constants. After *N*-re-acetylation and HPLC separation, we identified a major disaccharide that contained a GlcNAc α/β residue in terminal reducing position and DATDH as observed in the intact Ch HF-PS (supplemental Fig. S5). As expected, we observed the ^{1}H-^{1}H coupling constant pattern of DATDH after hydrolysis of the polysaccharide as S,L,S,S ($^{3}J_{H1,H2} \sim 3Hz$; $^{3}J_{H2,H3} \sim 8Hz$; $^{3}J_{H3,H4} \sim 3Hz$; $^{3}J_{H4,H5} \sim 3Hz$), which typified an α-*galacto* configuration. Furthermore, the presence of *N*-acetyl groups in C2 ($\delta_{H2\alpha/C2\alpha}$3.87/55.7, δ_{H2bC2} 3.68/58.5) and C4 ($\delta_{H4/C4}$ 4.30/54.8) as well as the methyl group in C6 ($\delta_{H1/C1}$ 1.13/16.9) permitted identification of this monosaccharide as an α-2,4,6 tri-deoxy-2,4-di-*N*-acetylated-galactosamine, commonly referred as α-FucdiNAc. The FucdiNAc in terminal nonreducing position was linked to the C6 position of the GlcNAc residue, as proved by the deshielded C6 carbon at 67.2 ppm and the H6,6′ resonances at 3.96 and 3.66 accordingly to results obtained from intact Ch HF-PS.

The sequence of the Ch HF-PS repeat unit was established essentially by the ^{13}C,^{1}H HMBC heteronuclear NMR experiment due to the observation of numerous extra-residual $^{3}J_{H,C}$ correlations (data not shown). Indeed, in accordance with the observation of the deshielded value of **III**-C6 at 66.61 ppm compared with 61 ppm for the free β-Glc*p*NAc residue, the strong **I**-H1/**III**-C6 correlation signal at 4.915/66.61 ppm on the HMBC spectrum established the sequence αFucdiNAc(1–6)Glc*p*NAcβ. Similarly, $^{3}J_{H,C}$ correlation between **III**-H1 and **II**-C6 at 4.599/68.19 ppm as well as the deshielding of **II**-C6 to 68.09 ppm established that the β-Glc*p*NAc **III** residue was linked to β-Gal*p* **II** in C6 position. Finally, the Glu-C2 chemical shift at 80.72 ppm and the **II**-H1/Glu-2 correlation signal demonstrated that the β-Gal*p* residue was linked to C2 position of glutarate group. This asymmetric carbon presented an (*R*) absolute configuration, as demonstrated by gas chromatography analysis compared with the 2-(*R*)-hydroxyglutarate standard (data not shown). In conclusion, the NMR analyses permitted definition of the structure of the repeating trisaccharide unit from charged polysaccharide Ch HF-PS as Gal*p*(α1-2)[2-R-hydroxyglutar-5ylamido(4)]-4,6-dideoxy-Gal*p*NAc(α1-6)Glc*p*NAc(β1–6).

MALDI-MS analysis of the Ch HF-PS in negative mode showed four sets of major signals at *m*/*z* 1381/1403, 2063/2085, 2745/2767, and 3428/3449 attributed to $[M-H]^-$/$[M-2H+Na]^-$ adducts of intact oligosaccharides containing two, three, four, and five repeating units, respectively (supplemental Fig. S6). Indeed, the difference of 682 mass units matches with the calculated composition of the trisaccharide, whose structure has been established by NMR, confirming the previous attribution. Furthermore, several sets of signals corresponding to partially truncated repeating units were observed along intact ones (supplemental Fig. S6).

Analysis of the Early Biofilm Phase Polysaccharide—After the total structural analysis of the two polysaccharides isolated from the planktonic phase, the structure of the early biofilm cell wall polysaccharide was established using identical methods. As shown in Fig. 2, *C* and *F*, the ^{13}C,^{1}H HSQC NMR spectrum of early biofilm polysaccharide was identical to the neutral polysaccharide Ne HF-PS isolated from the planktonic phase bacteria. This demonstrated that the cell wall polysaccharide isolated from bacteria in early phase of biofilm formation is constituted by a single polysaccharide with a [GlcNAc(β1–3)]GlcNAc(β1–6)[Glc(β1–3)][ManNAc(α1-4)]GalNAc(α1–4)ManNAc(β1–4) repeating unit.

Thus, the comparison of cell-wall polysaccharides from different phases established that *B. cereus* synthesizes different sets of polysaccharides depending on the phase of growth. A common polysaccharide constituted by the hexasaccharide [GlcNAc(β1–3)]GlcNAc(β1–6)[Glc(β1–3)][ManNAc(α1-4)]GalNAc(α1–4)ManNAc(β1–4) repeating unit (Ne HF-PS) was observed in both planktonic and biofilm phases at all time points observed. Conversely, another very unusual polysaccharide presenting a Gal*p*(α1–2)[2-R-hydroxyglutar-5ylamido(4)]-4,6-dideoxy-Gal*p*NAc(α1–6)Glc*p*NAc(β1–6) repeating unit (Ch HF-PS) appeared to be phase-specific. Indeed, this compound was observed in bacterial cell walls at every time point of planktonic cultures from 5 to 20 h as well as in biofilm from 72 to 96 h but totally disappeared in bacteria from early biofilms.

In Vivo Analysis of the Surface Polysaccharides by HR-MAS NMR—To rule out the possibility that the disappearance of Ch HF-PS may be linked to variations in the extraction procedure, we performed HR-MAS NMR analysis on total bacterial cells in each growth phase. This technique was effectively used to analyze the structure of glycosylated cell wall components, including mycobacterial and yeast polysaccharides, from intact living bacterial cells without proceeding to any purification procedure (39, 40). As previously shown, parameters of NMR signals originating from HR-MAS NMR experiments of total cell walls and from liquid NMR experiment of purified polysaccharides are strictly identical when experiments are run in similar experimental conditions, which permits direct identification of signals from HR-MAS based on liquid NMR analyses. Thus, based on data collected on purified polysaccharides, ^{13}C,^{1}H HSQC HR-MAS NMR spectrum of intact bacteria from the planktonic phase showed all the signals associated with both polysaccharides (Fig. 7 and supplemental Fig. S7). Interestingly, HSQC signals associated with Ch HF-PS (**I**, **II** and **III**) exhibited a much higher intensity than those associated with Ne HF-PS when compared with the liquid NMR spectrum of total polysaccharide isolated from the same growth phase. The relative lower responsiveness of Ne HF-PS to HR-MAS NMR was most probably the result of the specific feature of this technique that

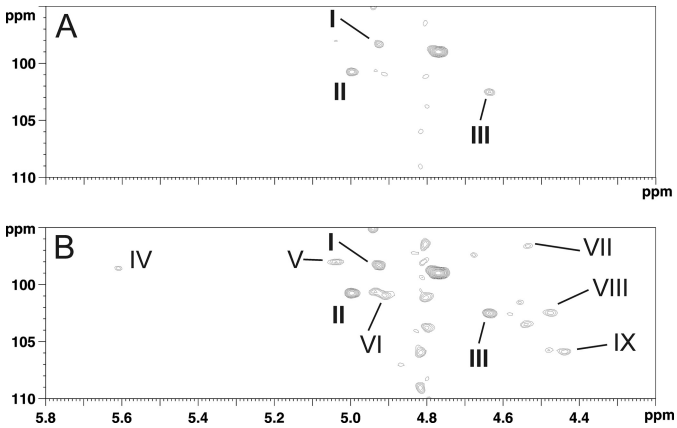

FIGURE 7. **Detail of the anomer region of ^{13}C,^{1}H HSQC HR-MAS NMR analysis of bacterial cell surface of *B. cereus* from planktonic phase of growth.** When looked at a low sensitivity, only signals from Ch HF-PS (**I** to **III**) can be seen (*A*), whereas increasing sensitivity permits to recover signals from Ne HF-PS (**IV** to **IX**) (*B*).

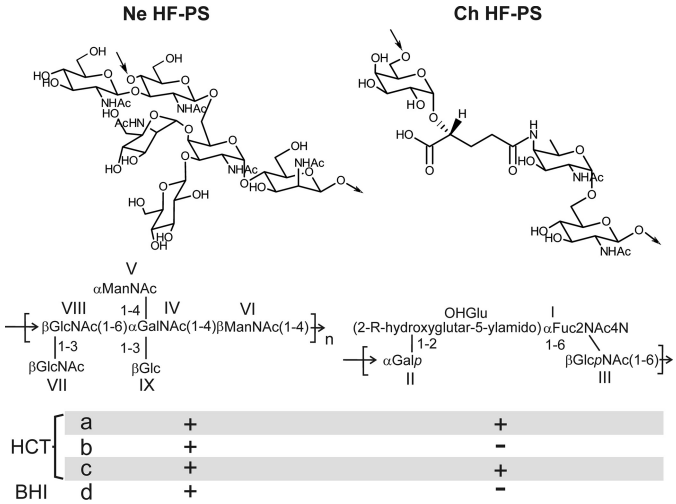

FIGURE 8. **Structure of HF-PS repetition units isolated from *B. cereus* strains ATCC and 14579.** Two unrelated polysaccharides, Ne HF-PS and Ch HF-PS, were identified from *B. cereus* 14579. Ne HF-PS is synthesized irrespective of the growing conditions, whereas Ch HF-PS synthesis is regulated along the biofilm formation and according to culture medium, HCT (poor medium) or BHI (rich medium). *a*, and *d*, planktonic phase; *b*, early biofilm formation (28–48 h); *c*, late biofilm formation (72–96 h).

suppresses the signal from constrained molecules that exhibit a short transversal relaxation time (T2). This provides a clear indication that the linear Ch HF-PS is more mobile and accessible at the bacterial cell surface than the branched Ne HF-PS. Conversely with the planktonic phase, an HR-MAS spectrum of early biofilm intact bacteria only showed signals associated to Ch HF-PS (data not shown). This set of data definitely established that the phenotypic differences that we observed between phases are not artifacts generated by multiple purification and chemical degradation steps of polysaccharides. Furthermore, it confirmed that Ch HF-PS was physically associated to bacteria cell surface along Ne HF-PS and not released in the culture medium.

Comparison of HF-PS from Bacteria Grown in Different Culture Media—Altogether, our experimental data unambiguously established that *B. cereus* ATCC 14579 was able to synthesize two secondary cell wall polysaccharides presenting totally different structures, Ne HF-PS and Ch HF-PS (Fig. 8). In their previous work, Leoff et al. (23, 24) did report the presence of Ne HF-PS polysaccharide in the *B. cereus* ATCC14579 without providing its full structure but conclusively established the fine structures of its equivalent in a wide panel of *B. cereus* strains (41). In contrast, these authors never mentioned the presence of an equivalent of Ch HF-PS in any *B. cereus* strain, including Bc 14579, or in *B. anthracis* (23–25, 27, 41). To rationalize such an important discrepancy between our respective data, we hypothesized that the production of Ch HF-PS might be dependent on the culture medium, as Leoff et al. (23, 24) used a rich medium (BHI), whereas we used a poor medium (HCT). As recently reported, *B. cereus* ATCC 14579 is capable of forming biofilm in poor medium culture conditions, whereas rich medium cannot sustain biofilm formation at any temperature (22). Thus, herein the choice of a poor medium for studying the qualitative modifications of surface polysaccharides was an absolute requirement. Assessment of the extraction and processing procedures of the HF-PS revealed some other potential sources of differences such as the heat inactivation of bacteria (121 °C for 1 h) before extraction and sonication steps that may lead to a loss in the acid labile Ch HF-PS (27). To find out the origin of the discrepancies between our respective observations and understand the precise conditions in which the synthesis of Ch HF-PS is promoted, we compared the polysaccharide composition of HF-PS extracted from bacteria grown in planktonic phases in different culture media, BHI or HCT. As observed on the comparative analysis of ^{1}H NMR spectra, total HF-PS isolated from bacteria grown in rich medium exclusively contained Ne HF-PS, whereas bacteria grown in poor medium synthesized both Ch HF-PS and Ne HF-PS (Fig. 9). Heat inactivation and sonication of bacteria grown in rich medium did not induce more structural differences (data not shown). This experiment unambiguously demonstrated that the synthesis of Ch HF-PS is strictly regulated by the culture conditions of bacteria. Altogether, our study showed that *B. cereus* strain ATCC 14579 displays two secondary cell wall polysaccharides in which syntheses are tightly regulated by 1) the culture conditions and 2) the culture phase.

DISCUSSION

Various polysaccharides covalently bound to the peptidoglycan have been described in Gram-positive bacteria (1). However, this is the first report of two different peptidoglycan-associated coexisting polysaccharides. We independently isolated from the *B. cereus* ATCC 14579 strain these polysaccharides using two totally different strategies. One strategy was based on the partial acid depolymerization and solubilization in a hydroalcoholic solution, which permitted differentiation of the two components according to their susceptibility to mild acid treatment. Five steps of mild hydrolysis enabled a total solubilization of the acid labile polysaccharide. Despite its total solubilization, the overall structure of this acid-labile polysaccharide was kept intact without gross modification, albeit a partial depolymerization (data not shown). Conversely, the acid-resistant fraction was totally insoluble after five rounds of mild acid hydrolysis,

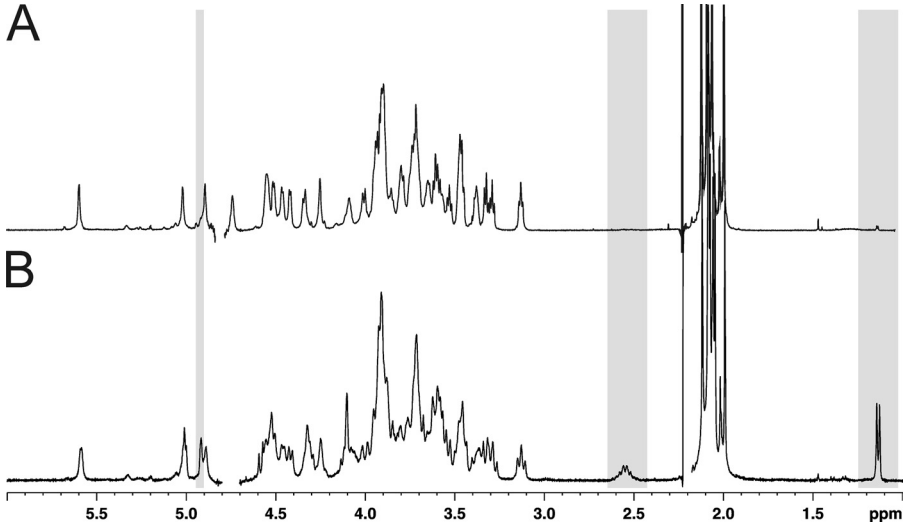

FIGURE 9. **Comparison of the HF-PS isolated from bacteria grown in different media.** ^{1}H-NMR spectra of HF-PS isolated from the planktonic phases of bacteria grown in rich medium (BHI) (*A*) and poor medium (HCT) (*B*).

which permitted the obtaining of two fractions devoid of cross contaminations. The two polysaccharides could also be separated without prior acid hydrolysis according to their charge on a strong anion exchange column. One neutral fraction (Ne HF-PS) corresponding to the acid-resistant polysaccharide and one charged fraction (Ch HF-PS) corresponding to the acid-labile fraction were purified that way.

The detailed structural analysis of individual polysaccharides provided in the present report established that these two polysaccharides were structurally unrelated. Their structures are summarized in Fig. 8. Neutral polysaccharide was composed of the major hexasaccharide repeat unit →4)[GlcNAc(β1-3)]GlcNAc(β1–6)[Glc(β1–3)][ManNAc(α1–4)]GalNAc(α1-4)ManNAc(β1→. Although the major repeating unit is fully substituted by βGlcNAc, βGlc, and αManNAc residues to form the hexasaccharide unit, the observation of minor NMR signals (data not shown) strongly suggested the presence of a slight heterogeneity in the branching pattern of the trisaccharide backbone →4)GlcNAc(β1–6)GalNAc(α1–4)ManNAc(β1→ due to non-stoichiometric substitutions of the backbone. The structure of the polysaccharide backbone that we have established fits well with the consensus sequence that was nicely defined by Leoff and co-workers by comparing the structures of HF-PS isolated from *B. anthracis* and *B. cereus* ATCC 10987 (24, 27). Indeed, the authors reported the exact structures of the polysaccharide backbones of HF-PS isolated from *B. anthracis* as →4)GlcNAc(β1–6)GlcNAc(α1–4)ManNAc(β1→ and from *B. cereus* ATCC 10987 as →4)GlcNAc(β1–6)GalNAc(α1-4)ManNAc(β1→. Based on these structural features and despite species-specific branching patterns by α-galactosidase and β-galactosidase residues, high similarity permitted the proposition of the potential consensus sequence βGlcNAc-αHexNAc-βManNAc for HF-PS in *Bacillus* species. As established by the present report, the trisaccharide backbones of *B. cereus* ATCC 14579 and *B. cereus* ATCC 10987 are similar, but the branching pattern of Ne HF-PS from ATCC 14579 is more complex than ATCC 10987 due to an abundant substitution by βGlcNAc, βGlc, and αManNAc residues (Fig. 8). However, in contrast to ATCC 10987, no data supported the presence of *O*-acetylation in the polysaccharide of *B. cereus* 14579.

Along these small scale species-specific differences between ATCC 14579 and ATCC 10987, the most striking feature of *B. cereus* ATCC 14579 was the observation of another, so far unidentified, stage-specific charged polysaccharide, Ch HF-PS. It was specifically released from bacteria by aqueous hydrogen fluoride treatment along Ne HF-PS and represented about 70% of the total HF-PS content of bacteria grown in planktonic phase. This polysaccharide exhibited a very unusual repeating unit →6)Gal(α1–2)(2-R-hydroxyglutar-5-ylamido)Fuc2NAc4N(α1–6)GlcNAc(β1→ so far never identified in the *Bacillus* genus. HR-MAS NMR analysis of the intact bacteria demonstrated that this component was associated to its cell surface. Furthermore, comparison of the NMR data originating from liquid and HR-MAS experiments strongly suggested that this component was part of the outmost layer surrounding the bacteria. Even more surprising and in contrast to Ne HF-PS, the expression profile of Ch HF-PS dramatically changed along the bacterial growth and according to the culture medium in which bacteria were grown. The fact that it is exclusively expressed at the surface of bacteria grown in poor culture medium explains the apparent discrepancy of our results compared with previous studies (24). One may easily speculate that the expression of Ch HF-PS in poor medium is somehow correlated to the biofilm formation capacity of *B. cereus* ATCC 14579 (22). Correlation between biofilm formation and SCWP polysaccharides is further substantiated by the fact that Ch HF-PS surface expression is also regulated along the biofilm formation. Indeed, whereas Ch HF-PS was observed at every point of the bacterial growth in planktonic phase, it could only be observed in later cultures (from 72 h) of biofilm phase, the earlier cultures being totally devoid of Ch HF-PS. It is noteworthy that peptidoglycan is not modified during the biofilm phase, suggesting that the structural bacterial cell wall is only

changed by the covalently associated polysaccharides (data not shown). And, as SLH proteins are anchored to the HF-PS (3), any change in the HF-PS composition may result in changes in cell surface proteins.

As Ch HF-PS is not required for biofilm initiation and early development, it is unlikely to play a role in cell-substrate interaction or in cell-cell interaction within the biofilm. However, high quantities of extracellular DNA were found in the *B. cereus* biofilm matrix (42). The negatively charged backbone of this extracellular DNA might interact more easily with bacterial cell surfaces devoid of negatively charged polysaccharide, causing an increase of the biofilm cohesion. The interaction between extracellular DNA and surface polysaccharides was supported by the observation that deletion of genes likely to be involved in extracellular DNA production impaired biofilm formation in *B. cereus*, but this hypothesis still awaits definitive experimental proof (42). In planktonic cultures, Ch HF-PS could be involved in the bacterium protection against environmental stresses, for instance by sequestering positively charged antimicrobial agents. This putative role of Ch HF-PS would not be required in biofilms, as the matrix was shown to act as an efficient shield against various environmental stresses (43). The appearance of Ch HF-PS in aging biofilms could be attributed to biofilms cells switching back to a planktonic state of growth while still located within the biofilm. Aged biofilms are prone to dispersal and include a leaving bacterial subpopulation showing important phenotypic changes (44). In addition, the co-existence of bacteria in various growth states was shown to occur within *B. subtilis* biofilms (45).

In conclusion, the identification of a new tightly regulated surface component in *B. cereus* 14579 offers new insights into the comprehension of the mechanisms that control adhesion and biofilm formation. Although the exact nature of the relationships between SCWP polysaccharide and biofilm formation are still unclear, we believe that our study will provide solid structural bases for the functional analysis of this new polysaccharide. Furthermore, the induction of this new SCWP polysaccharide in specific culture conditions points to the possibility that other, still unknown SCWP polysaccharides could be induced in other environmental conditions, such as the host internal milieu. Changes in the *B. cereus* cell wall polysaccharides components could be involved in the high adaptability of this bacterium to environmental changes.

Acknowledgments—We thank I. G. Boneca from the Institut Pasteur for the analysis of peptidoglycans by HPLC, B. Coddeville from Unité de Glycobiologie Structurale et Fonctionnelle for helping in the MS/MS analysis of polysaccharides, and Prof. A. Dell for providing access to mass spectrometry facility (Division of Molecular Biosciences, Faculty of Natural Sciences, Imperial College London). The 800- and 900-MHz spectrometers were funded by Région Nord-Pas de Calais, European Union (FEDER), Ministère Français de la Recherche, Université Lille1-Sciences and Technologies, and CNRS. The 400 MHz facility was funded by the Centre Commun de Mesure RMN de l'Université de Lille1.

REFERENCES

1. Vollmer, W. (2008) *FEMS Microbiol. Rev* **32,** 287–306
2. Weidenmaier, C., Peschel, A., Xiong, Y. Q., Kristian, S. A., Dietz, K., Yeaman, M. R., and Bayer, A. S. (2005) *J. Infect. Dis.* **191,** 1771–1777
3. Mesnage, S., Fontaine, T., Mignot, T., Delepierre, M., Mock, M., and Fouet, A. (2000) *EMBO J.* **19,** 4473–4484
4. Chitlaru, T., Ariel, N., Zvi, A., Lion, M., Velan, B., Shafferman, A., and Elhanany, E. (2004) *Proteomics* **4,** 677–691
5. Gohar, M., Gilois, N., Graveline, R., Garreau, C., Sanchis, V., and Lereclus, D. (2005) *Proteomics* **5,** 3696–3711
6. Antikainen, J., Anton, L., Sillanpää, J., and Korhonen, T. K. (2002) *Mol. Microbiol.* **46,** 381–394
7. Sára, M., and Sleytr, U. B. (2000) *J. Bacteriol.* **182,** 859–868
8. Moscoso, M., García, E., and López, R. (2006) *J. Bacteriol.* **188,** 7785–7795
9. Götz, F. (2002) *Mol. Microbiol.* **43,** 1367–1378
10. Lebeer, S., Verhoeven, T. L., Perea Vélez, M., Vanderleyden, J., and De Keersmaecker, S. C. (2007) *Appl. Environ. Microbiol.* **73,** 6768–6775
11. Kolter, R. (2005) *Trends Microbiol.* **13,** 1–2
12. Davey, M. E., and O'toole, G. A. (2000) *Microbiol. Mol. Biol. Rev* **64,** 847–867
13. Whitchurch, C. B., Tolker-Nielsen, T., Ragas, P. C., and Mattick, J. S. (2002) *Science* **295,** 1487
14. Peng, J. S., Tsai, W. C., and Chou, C. C. (2002) *Int. J. Food Microbiol.* **77,** 11–18
15. Auger, S., Ramarao, N., Faille, C., Fouet, A., Aymerich, S., and Gohar, M. (2009) *Appl. Environ. Microbiol.* **75,** 6616–6618
16. Ren, D., Bedzyk, L. A., Setlow, P., Thomas, S. M., Ye, R. W., and Wood, T. K. (2004) *Biotechnol. Bioeng.* **86,** 344–364
17. Lee, K., Costerton, J. W., Ravel, J., Auerbach, R. K., Wagner, D. M., Keim, P., and Leid, J. G. (2007) *Microbiology* **153,** 1693–1701
18. Hsueh, Y. H., Somers, E. B., Lereclus, D., and Wong, A. C. L. (2006) *Appl. Environ. Microbiol.* **72,** 5089–5092
19. Kotiranta, A., Lounatmaa, K., and Haapasalo, M. (2000) *Microbes Infect.* **2,** 189–198
20. Bottone, E. J. (2010) *Clin. Microbiol. Rev.* **23,** 382–398
21. Gohar, M., Faegri, K., Perchat, S., Ravnum, S., Økstad, O. A., Gominet, M., Kolstø, A. B., and Lereclus, D. (2008) *PLoS ONE* **3,** e2793
22. Wijman, J. G., de Leeuw, P. P., Moezelaar, R., Zwietering, M. H., and Abee, T. (2007) *Appl. Environ. Microbiol.* **73,** 1481–1488
23. Leoff, C., Saile, E., Rauvolfova, J., Quinn, C. P., Hoffmaster, A. R., Zhong, W., Mehta, A. S., Boons, G. J., Carlson, R. W., and Kannenberg, E. L. (2009) *Glycobiology* **19,** 665–673
24. Leoff, C., Choudhury, B., Saile, E., Quinn, C. P., Carlson, R. W., and Kannenberg, E. L. (2008) *J. Biol. Chem.* **283,** 29812–29821
25. Leoff, C., Saile, E., Sue, D., Wilkins, P., Quinn, C. P., Carlson, R. W., and Kannenberg, E. L. (2008) *J. Bacteriol.* **190,** 112–121
26. Archibald, A. R., Hancock, I. C., and Harwood, C. R. (1993) in *Bacillus Subtilis and Other Gram-Positive Bacteria* (Sonenshein, A. L., Hoch, J. A., and Losick, R., eds) pp. 381–410, American Society for Microbiology Press, Washington, D. C.
27. Choudhury, B., Leoff, C., Saile, E., Wilkins, P., Quinn, C. P., Kannenberg, E. L., and Carlson, R. W. (2006) *J. Biol. Chem.* **281,** 27932–27941
28. Lang, W. K., Glassey, K., and Archibald, A. R. (1982) *J. Bacteriol.* **151,** 367–375
29. Lecadet, M. M., Blondel, M. O., and Ribier, J. (1980) *J. Gen. Microbiol.* **121,** 203–212
30. Houry, A., Briandet, R., Aymerich, S., and Gohar, M. (2010) *Microbiology* **156,** 1009–1018
31. Candela, T., and Fouet, A. (2005) *Mol. Microbiol.* **57,** 717–726
32. Ciucanu, I., and Kerek, F. (1984) *Carbohydr. Res.* **131,** 209–217
33. Guerardel, Y., Czeszak, X., Sumanovski, L. T., Karamanos, Y., Popescu, O., Strecker, G., and Misevic, G. N. (2004) *J. Biol. Chem.* **279,** 15591–15603
34. Zuiderweg, E. R. (2002) *Biochemistry* **41,** 1–7
35. Koërner, T. A., Prestegard, J. H., and Yu, R. K. (1987) *Methods Enzymol.* **138,** 38–59
36. Bradbury, J. H., and Jenkins, G. A. (1984) *Carbohydr. Res.* **126,** 125–156

37. Stimson, E., Virji, M., Makepeace, K., Dell, A., Morris, H. R., Payne, G., Saunders, J. R., Jennings, M. P., Barker, S., and Panico, M. (1995) *Mol. Microbiol.* **17,** 1201–1214
38. Vinogradov, E., MacLean, L. L., Crump, E. M., Perry, M. B., and Kay, W. W. (2003) *Eur. J. Biochem.* **270,** 1810–1815
39. Lee, R. E., Li, W., Chatterjee, D., and Lee, R. E. (2005) *Glycobiology* **15,** 139–151
40. Maes, E., Mille, C., Trivelli, X., Janbon, G., Poulain, D., and Guérardel, Y. (2009) *J. Biochem.* **145,** 413–419
41. Forsberg, L. S., Choudhury, B., Leoff, C., Marston, C. K., Hoffmaster, A. R., Saile, E., Quinn, C. P., Kannenberg, E. L., and Carlson, R. W. (2011) *Glycobiology* **21,** 934–948
42. Vilain, S., Pretorius, J. M., Theron, J., and Brözel, V. S. (2009) *Appl. Environ. Microbiol.* **75,** 2861–2868
43. Flemming, H. C., and Wingender, J. (2010) *Nat. Rev. Microbiol.* **8,** 623–633
44. Karatan, E., and Watnick, P. (2009) *Microbiol. Mol. Biol. Rev.* **73,** 310–347
45. Lopez, D., Vlamakis, H., and Kolter, R. (2009) *FEMS Microbiol. Rev.* **33,** 152–163